

Resonant Interaction between Localized and Extended Vibrational Modes in Si: ^{18}O under Pressure

L. Hsu,^{1,*} M. D. McCluskey,^{1,2,†} and J. L. Lindström³

¹*Department of Physics, Washington State University, Pullman, Washington 99164-2814*

²*Institute for Shock Physics, Washington State University, Pullman, Washington 99164-2816*

³*Department of Physics, Division of Solid State Physics, Lund University, S-221 00 Lund, Sweden*

(Received 15 November 2002; published 7 March 2003)

The interaction between localized and extended vibrational modes in solids is of central importance in understanding how local vibrational modes decay into phonons. Interstitial oxygen (O_i) in silicon is a model system for studying such interactions. Using hydrostatic pressure, we have brought the antisymmetric stretch mode of $^{18}\text{O}_i$ in silicon into resonance with the second harmonic of the $^{18}\text{O}_i$ resonant mode. Infrared spectroscopy was used to observe an anticrossing between these two vibrational modes at pressures near 4 GPa. A model of the interaction between these modes produced excellent agreement with the experimentally observed frequencies and linewidths.

DOI: 10.1103/PhysRevLett.90.095505

PACS numbers: 63.20.Pw

Oxygen is one of the most common and technologically important impurities found in Czochralski-grown silicon [1]. In as-grown crystals, oxygen occurs principally as an interstitial defect (O_i) [2,3]. The oxygen atom is bound to two nearest-neighbor silicon atoms and is found in the off-bond-center position. Because the structure of O_i is well understood, it is an ideal system for studying interactions between localized and extended vibrational modes. Such interactions are of central importance in understanding vibrational lifetimes of defects in semiconductors, an area of intense interest [4–6].

Over the past few decades, the local vibrational modes (LVMs) of interstitial oxygen have been measured and different models developed to account for their origins [7–12]. The most well-known vibrational mode is found at 1136 cm^{-1} and corresponds to the oscillation of a $^{16}\text{O}_i$ atom along the [111] direction, out of phase with the two silicon atoms to which it is bonded [13]. This vibrational excitation is known as the antisymmetric *stretch* mode. Isotope studies have located the corresponding modes for $^{17}\text{O}_i$ and $^{18}\text{O}_i$ [7], in addition to those due to different isotopic combinations of nearest-neighbor silicon atoms. Other $^{16}\text{O}_i$ -related modes include the *transverse* mode at 29 cm^{-1} , corresponding to movement of the oxygen atom in the [111] plane [14], and the *resonant* mode at 517 cm^{-1} [15], which involves the transverse motion of the neighboring silicon atoms [11]. Unlike the stretch mode, the resonant mode is extended spatially, with many neighboring silicon atoms participating in the vibrational motion.

In this study, we have used hydrostatic pressure to bring the 1084 cm^{-1} stretch mode of $^{18}\text{O}_i$ into resonance with a second harmonic of the 517 cm^{-1} resonant mode. The interaction between the two modes results in an anticrossing of the frequencies. This is the first reported instance of a pressure-induced interaction between a localized and an extended vibrational mode. Since the frequency of the resonant mode lies within the continuum of lattice two-

phonon states, this interaction also provides information regarding the decay of LVMs into lattice phonons. Such knowledge is useful because vibrational relaxation mechanisms affect properties such as diffusion and energy transfer involving oxygen impurities in silicon [16].

We used a piston-cylinder diamond-anvil cell with type IIA diamonds to generate pressures up to 6.3 GPa. The Si samples, which contained $\sim 10^{18}\text{ cm}^{-3}$ of ^{18}O , were small squares approximately $200\text{ }\mu\text{m}$ on a side polished to a thickness of $50\text{ }\mu\text{m}$. Nitrogen was used as the pressure medium and the cell was loaded using the liquid immersion technique [17]. To determine the pressure in the cell at liquid-helium temperatures, we measured the frequencies of the ν_3 vibrational modes of both N_2 and CO_2 in the nitrogen medium [18]. The diamond-anvil cell was placed in a Janis STVP continuous-flow liquid-helium cryostat with wedged ZnSe windows and kept at a temperature of 8 K during data collection. A Bomem DA8 vacuum Fourier transform spectrometer with a KBr beam splitter was used to obtain infrared absorption spectra ranging from 500 to 5000 cm^{-1} with a resolution of $\geq 1\text{ cm}^{-1}$. An off-axis parabolic mirror and light-concentrating cone were mounted in front of the cell and a Ge:Cu photoconductive detector [19] was placed directly behind the cell.

Figure 1 shows IR absorption spectra of the $^{18}\text{O}_i$ LVM. Near atmospheric pressure, four distinct peaks can be seen, all of which have been observed previously [7]. The highest energy peak (I) corresponds to a transition $|l=0, N=0\rangle \rightarrow |l=0, N=1\rangle$, where l is the angular momentum about the [111] axis and N is the longitudinal (stretch) quantum number. The two smaller peaks next highest in energy correspond to the same transition, but with the $^{18}\text{O}_i$ atom bound to combinations of less common Si isotopes. The lowest energy peak (II) corresponds to a $|l=\pm 1, N=0\rangle \rightarrow |l=\pm 1, N=1\rangle$ transition. At high pressures, the frequencies of the two transitions

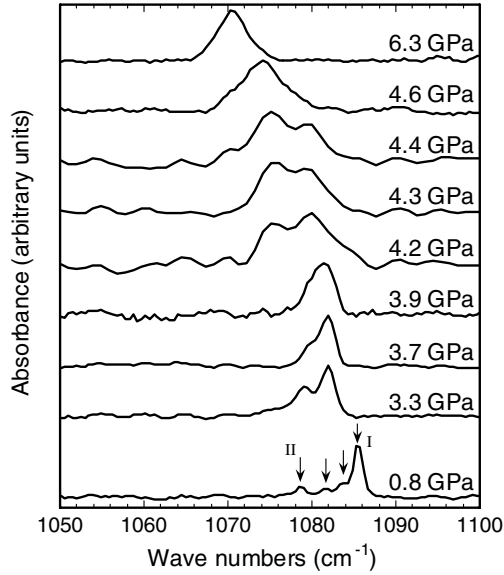


FIG. 1. Absorption peaks due to stretch-mode LVMs in $\text{Si:}^{18}\text{O}_i$ at several pressures. Peaks I and II correspond to the $|l=0, N=0\rangle \rightarrow |l=0, N=1\rangle$ and $|l=\pm 1, N=0\rangle \rightarrow |l=\pm 1, N=1\rangle$ transitions, respectively. An anticrossing between the $^{18}\text{O}_i$ stretch mode (upper peak) and the second harmonic of the $^{18}\text{O}_i$ resonant mode (lower peak) can be seen above 3.9 GPa.

become nearly degenerate and only a single broad peak is observed.

At intermediate pressures (3.3–4.6 GPa), the $^{18}\text{O}_i$ LVM shows unusual behavior. At the low end of this range, the two peaks (I and II) are seen merging, as was previously observed for the $^{16}\text{O}_i$ LVM [20]. However, around 4.2 GPa, a second absorption peak appears on the low-energy shoulder of the merged LVM peaks. As the pressure is increased, this peak grows in size and the peak due to the merged LVMs disappears above 4.4 GPa. In obtaining the spectra for this study, the cell pressure was increased and decreased several times, with no evidence of hysteresis. Figure 2 shows a plot of the frequencies of the observed peaks for both $^{16}\text{O}_i$ and $^{18}\text{O}_i$ throughout the entire pressure range studied. The dotted and solid lines are frequencies generated by the theoretical model, as discussed in the following paragraphs. The peaks associated with $\text{Si:}^{16}\text{O}_i$ show a smooth, continuous shift with pressure. However, for the $\text{Si:}^{18}\text{O}_i$ peaks, there is an avoided crossing around 4 GPa. This anticrossing behavior is the result of a resonant interaction between the $^{18}\text{O}_i$ stretch mode and a second harmonic of the 517 cm^{-1} resonant mode [21].

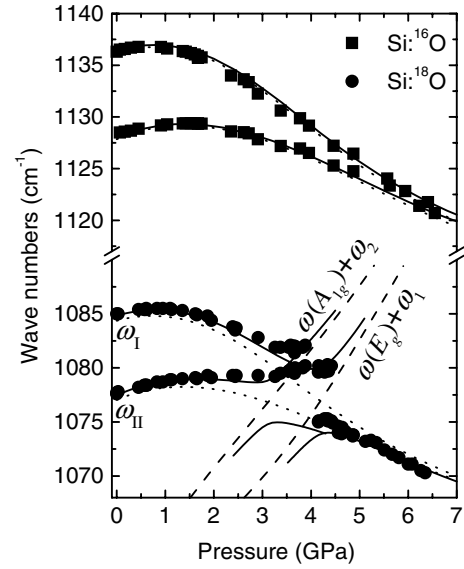


FIG. 2. Plot of the frequencies of the $^{18}\text{O}_i$ and $^{16}\text{O}_i$ vibrational modes in Si. The dotted lines are plots of ω_I and ω_{II} [Eq. (4)]. The dashed lines are plots of combination modes [Eqs. (3) and (8)]. The solid lines are frequencies obtained from the theoretical model of the interaction between the stretch and combination modes [Eq. (7)].

To model the experimental observations, we use the approach described by McCluskey and Haller [20] to calculate the frequencies of peaks I and II. In this model, the O_i potential in the [111] plane [9] varies with pressure such that the oxygen buckles outward as pressure is applied. We use that same potential, $V(r)$, in this study. Assuming cylindrical symmetry, the wave function in the [111] plane is given by

$$\psi_l = u_l(r)e^{il\theta}, \quad (1)$$

where the radial wave function $u_l(r)$ and energy eigenvalues E are obtained by numerically solving the Schrödinger equation:

$$-\frac{\hbar^2}{2m} \left[\frac{1}{r} \frac{d}{dr} \left(r \frac{d}{dr} \right) - \frac{l^2}{r^2} \right] u_l(r) + V(r)u_l(r) = Eu_l(r), \quad (2)$$

where m is the mass of ^{16}O or ^{18}O . The energy differences between vibrational levels are defined

$$\omega_j \equiv (E_{l=j} - E_{l=j-1})/\hbar \quad (j = 1, 2). \quad (3)$$

The stretch-mode frequencies are given by [20]

$$\begin{aligned} \omega_I &= (m_{16}/m)^p (\omega_{s0} + \gamma P) + (m_{16}/m)^q (-\alpha' \langle r^2 \rangle_{l=0} + \beta' \langle r^4 \rangle_{l=0}), \\ \omega_{II} &= (m_{16}/m)^p (\omega_{s0} + \gamma P) + (m_{16}/m)^q (-\alpha' \langle r^2 \rangle_{l=1} + \beta' \langle r^4 \rangle_{l=1}), \end{aligned} \quad (4)$$

where m_{16} is the mass of ^{16}O , P is the pressure in GPa, and $\langle r^2 \rangle$ and $\langle r^4 \rangle$ are calculated from the wave function $u_l(r)$. The empirical exponents p and q describe the mass dependence and γ accounts for the slight pressure dependence of the

stretch-mode frequency due to compression of the Si-O bond. The parameters that give the best fit to the experimental data are listed in Table I. The frequencies obtained from Eq. (4) are plotted as the dotted lines in Fig. 2.

To model the anticrossing behavior observed for $^{18}\text{O}_i$, it is necessary to account for the interaction between the stretch mode and the resonant mode. A schematic diagram of the energy levels in this system is given in Fig. 3. In the D_{3d} symmetry of this defect, the stretch (ω_1) and resonant modes have A_{2u} and E_u symmetries, respectively. The second harmonics ($n=2$) of the resonant mode have A_{1g} and E_g symmetries, neither of which interacts with the ω_1 mode. However, the combination of an $|n=2, E_g\rangle$ and $|l=1\rangle$ mode is represented by $E_g \otimes E_u = A_{1u} \oplus A_{2u} \oplus E_u$, which contains an A_{2u} component. Hence, this combination mode interacts with the ω_1 mode. The matrix element describing this interaction is given by

$$A \equiv \langle l=1, N=0, n=2 | H | l=0, N=1, n=0 \rangle, \quad (5)$$

where n is the resonant-mode quantum number and H is the Hamiltonian. The symmetry of the ω_{II} mode is E_g . The combination of a $|n=2, A_{1g}\rangle$ and $|l=2\rangle$ mode is represented by $A_{1g} \otimes E_g = E_g$, so that this combination mode interacts with the ω_{II} mode [22]. The matrix element describing this interaction is given by

$$B \equiv \langle l=2, N=0, n=2 | H | l=1, N=1, n=0 \rangle. \quad (6)$$

The Hamiltonian for these interactions may be separated into two irreducible matrices,

$$H_1 = \begin{bmatrix} \omega_1 + i\Gamma_1 & A \\ A & \omega(E_g) + \omega_1 + i\Gamma_2 \end{bmatrix},$$

$$H_2 = \begin{bmatrix} \omega_{\text{II}} + i\Gamma_1 & B \\ B & \omega(A_{1g}) + \omega_2 + i\Gamma_2 \end{bmatrix}, \quad (7)$$

where $\omega(E_g)$ and $\omega(A_{1g})$ are the frequencies of the $|n=$

TABLE I. Parameters used to model the frequencies and linewidths for Si: $^{16}\text{O}_i$ and Si: $^{18}\text{O}_i$ under pressure [Eqs. (4), (7), and (8)].

Parameter	Value
α'	$237 \text{ cm}^{-1}/\text{\AA}^2$
β'	$170 \text{ cm}^{-1}/\text{\AA}^4$
ω_{s0}	1151.5 cm^{-1}
γ	$2.5 \text{ cm}^{-1}/\text{GPa}$
p	0.406
q	0.895
Γ_1	0.505 cm^{-1}
Γ_2	5 cm^{-1}
A	3.8 cm^{-1}
B	3.0 cm^{-1}
$\delta\omega(E_g)$	6 cm^{-1}
$\delta\omega(A_{1g})$	11 cm^{-1}

$2, E_g\rangle$ and $|n=2, A_{1g}\rangle$ modes, respectively; Γ_1 and Γ_2 are vibrational decay rates [23]. The energies in H_1 and H_2 are expressed relative to the ground state and the $|l=1, N=0\rangle$ level, respectively.

At zero pressure, the resonant mode has a frequency of 517 cm^{-1} . If we assume that the pressure dependence of this mode is equal to that of the Raman phonon [24], then the $n=2$ modes are given by

$$\omega(\Gamma) = 2 \times [517 \text{ cm}^{-1} + (5.2 \text{ cm}^{-1}/\text{GPa})P - (0.07 \text{ cm}^{-1}/\text{GPa}^2)P^2] - \delta\omega(\Gamma), \quad (8)$$

where $\Gamma = E_g$ or A_{1g} and $\delta\omega(\Gamma)$ is an anharmonic correction. The frequencies are given by the real parts of the eigenvalues of the matrices [Eq. (7)] and are plotted in Fig. 2 as solid lines. The frequencies of the combination modes are shown by the dashed lines. The pressure-dependent behavior of $^{16}\text{O}_i$ and $^{18}\text{O}_i$ is well described by this model.

In addition to describing the frequencies of the stretch modes, our model also reproduces the peak widths. The full width at half maxima (FWHM) for the ω_1 peaks, on the upper and lower branches of the avoided crossing, are plotted in Fig. 4. Whereas the width of the $^{16}\text{O}_i$ peak remains fairly constant over the entire pressure range [20], the $^{18}\text{O}_i$ peak exhibits an abrupt broadening at 4 GPa. The simulated widths were obtained from the imaginary parts of the eigenvalues of the matrices [Eq. (7)]. For pressures greater than 4 GPa, the ω_1 mode lies within the two-phonon density of states. Since the local density of states is roughly flat for frequencies below the resonant mode [25], the linewidth should increase by a fixed amount when the mode enters the two-phonon continuum [26]. To account for this effect, the FWHM for modes on the lower branch were adjusted upward by a fixed amount (3 cm^{-1}). The simulated FWHM values obtained by this approach are shown by the solid lines in Fig. 4. The initial increase in the FWHM at 4 GPa is caused by the interaction with the resonant mode, whereas the relatively constant FWHM for pressures greater than 5 GPa is due to the two-phonon continuum.

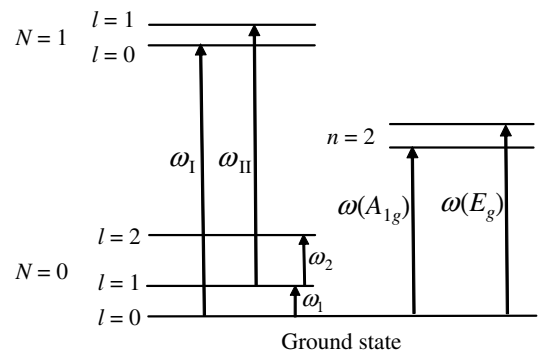


FIG. 3. Schematic diagram showing important vibrational levels of Si: O_i . The stretch-mode levels are shown on the left and the second-harmonic resonant modes are on the right.

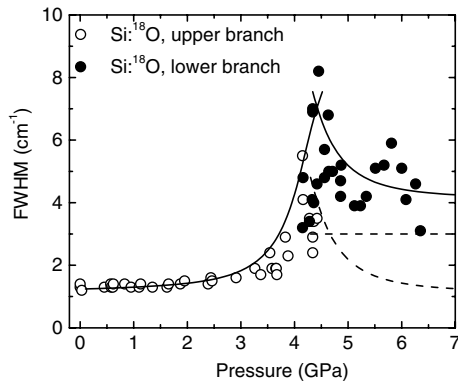


FIG. 4. Plot of the $^{18}\text{O}_i$ LVM linewidth in Si. The solid lines are plots of the widths calculated from our model. At high pressures, broadening due to interactions with the resonant mode (curved dashed line) and two-phonon continuum (flat dashed line) are shown separately.

The contributions from these two interactions are shown as dashed lines in Fig. 4.

In conclusion, we have used hydrostatic pressure to tune the frequency of an LVM into resonance with a spatially extended vibrational mode and used IR spectroscopy to observe the interaction between the two modes. By modeling the anticrossing behavior, we determined that the stretch mode (ω_I) and resonant mode interact with a coupling strength of $A = 3.8 \text{ cm}^{-1}$. When the two modes are in resonance, therefore, the stretch mode should transform into a resonance mode in ~ 4 ps. Such a transition from a localized to an extended mode is the first step toward decay into lattice phonons.

This work was supported by the National Science Foundation under Grant No. DMR-0203832. Support was also provided by WSU's Institute for Shock Physics through the DOE, Grant No. DE-FG03-97SF21388.

*Permanent address: General College, University of Minnesota, Minneapolis, MN 55455.

†Corresponding author.

Email address: mattmcc@wsu.edu

- [1] See *Semiconductors and Semimetals*, edited by F. Shimura (Academic, New York, 1994), Vol. 42, and references therein.
- [2] L. Jastrzebski, P. Zanzucchi, D. Thebault, and J. Lagowski, *J. Electrochem. Soc.* **129**, 1638 (1982).
- [3] B. Pajot, H.J. Stein, B. Cales, and C. Naud, *J. Electrochem. Soc.* **132**, 3034 (1985).

- [4] M. Budde, G. Lüpke, C. Parks Cheney, N. H. Tolk, and L. C. Feldman, *Phys. Rev. Lett.* **85**, 1452 (2000).
- [5] M. Budde, G. Lüpke, E. Chen, X. Zhang, N. H. Tolk, L. C. Feldman, E. Tarhan, A. K. Ramdas, and M. Stavola, *Phys. Rev. Lett.* **87**, 145501 (2001).
- [6] G. Lüpke, X. Zhang, B. Sun, A. Fraser, N. H. Tolk, and L. C. Feldman, *Phys. Rev. Lett.* **88**, 135501 (2002).
- [7] B. Pajot, in Ref. [1], pp. 191–249.
- [8] R. Jones, A. Umerski, and S. Öberg, *Phys. Rev. B* **45**, 11 321 (1992).
- [9] H. Yamada-Kaneta, C. Kaneta, and T. Ogawa, *Phys. Rev. B* **42**, 9650 (1990).
- [10] H. Yamada-Kaneta, *Physica (Amsterdam)* **308–310B**, 309 (2001).
- [11] J. Coutinho, R. Jones, P.R. Briddon, and S. Öberg, *Phys. Rev. B* **62**, 10 824 (2000).
- [12] T. Hallberg, L.I. Murin, J.L. Lindström, and V.P. Markevich, *J. Appl. Phys.* **84**, 2466 (1998).
- [13] H.J. Hrostowski and R.H. Kaiser, *Phys. Rev.* **107**, 966 (1957).
- [14] D.R. Bosomworth, W. Hayes, A.R.L. Spray, and G.D. Watkins, *Proc. R. Soc. London A* **317**, 133 (1970).
- [15] M. Stavola, *Appl. Phys. Lett.* **44**, 514 (1984).
- [16] M. Ramamoorthy and S. Pantelides, *Phys. Rev. Lett.* **76**, 267 (1996).
- [17] D. Schiferl, D.T. Cromer, and R.L. Mills, *High Temp. - High Pressures* **10**, 493 (1978).
- [18] M.D. McCluskey, L. Hsu, L. Wang, and E.E. Haller, *Phys. Rev. B* **54**, 8962 (1996).
- [19] Haller-Beeman and Associates (www.haller-beeman.com).
- [20] M.D. McCluskey and E.E. Haller, *Phys. Rev. B* **56**, 9520 (1997).
- [21] Resonant interactions involving hydrogen LVMS in silicon have been observed. See J.-F. Zheng and M. Stavola, *Phys. Rev. Lett.* **76**, 1154 (1996).
- [22] The ω_{II} mode can also interact with the $|n=2, E_g\rangle$ mode. However, in our model, these modes would intersect at ~ 5 GPa, at which point the ω_{II} peak is obscured by the ω_I peak.
- [23] The matrices in Eq. (7) describe coupled, damped oscillators, which may be treated classically. See, for example, K.N. Tong, *Theory of Mechanical Vibration* (Wiley, New York, 1960), pp. 114–118. In the limit of weak coupling, the FWHM values for the modes are given by $2\Gamma_1$ and $2\Gamma_2$, respectively.
- [24] B.A. Weinstein and G.J. Piermarini, *Phys. Rev. B* **12**, 1172 (1975).
- [25] E. Artacho, A. Lizón-Nordström, and F. Ynduráin, *Phys. Rev. B* **51**, 7862 (1995).
- [26] R.C. Newman *et al.*, *Mater. Sci. Forum* **258–263**, 1 (1997).